Post-Translational Modification

DOI: 10.1002/anie.201102542

Dynamic Monitoring of Newly Synthesized Proteomes: Up-Regulation of Myristoylated Protein Kinase A During Butyric Acid Induced Apoptosis**

*Kai Liu, Peng-Yu Yang, Zhenkun Na, and Shao Q. Yao**

Post-translational modification (PTM) is a highly dynamic yet precisely controlled process by which most eukaryotic proteins are chemically diversified.[1] Many critical cellular responses are mediated through PTMs, which lead to modulation of enzyme activity, protein conformation, protein–protein interaction, and cellular localization. Analysis of these modifications at the proteome level could provide invaluable biological insight but remains a technically challenging undertaking. Traditionally, PTMs have been studied by standard molecular biology techniques involving tedious isolation of individual proteins and subsequent direct detection and analysis of amino acids bearing the modification. Recent advances in mass spectrometry, when combined with stable-isotope or metabolic labeling approaches, have enabled several large-scale studies of PTMs and their dynamics.[2–4] These methods, however, analyze PTM changes of all proteins (old and new) present in the cell at the time of sampling and thus are only able to evaluate PTM dynamics at the ensemble level.[4,5] With unnatural metabolic building blocks and in vivo compatible conjugation chemistries becoming increasingly available (Scheme 1),[6,7] we sought to develop a proteomic strategy for the detection and identification of newly synthesized proteomes and their PTMs (Figure 1). We envisioned several advantages of studying the PTM dynamics of newly synthesized proteomes: 1) this method decreases the complexity of the proteome and enables the identification of PTM changes that occur in a predefined protein synthesis window; 2) it gives an accurate estimate of the time scale of different PTM events in transforming newly synthesized, modification-free proteins into mature functional entities; 3) it permits PTM analysis of primary protein synthesis responses to internal and external cues. To isolate a newly synthesized proteome, we made use of

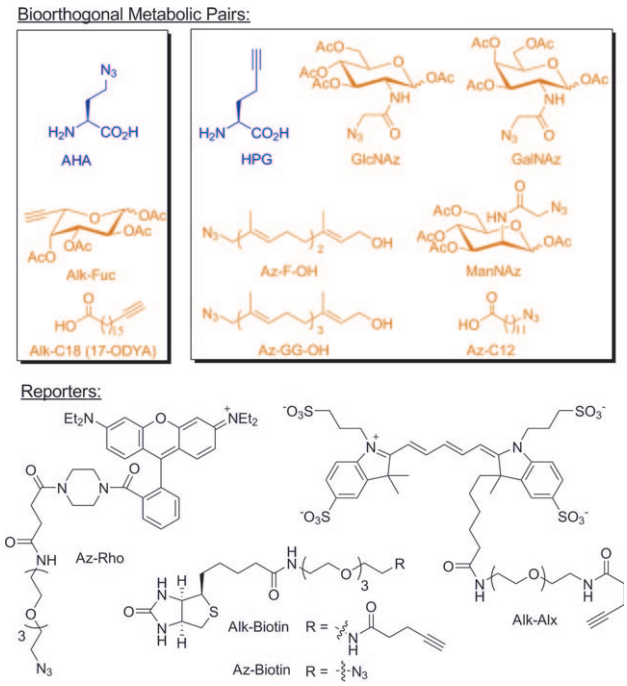

Scheme 1. Methionine surrogates (blue) and unnatural metabolite PTM probes (orange) form bio-orthogonal pairs for compatible double metabolic incorporation. Those forming pairs are boxed in the same group. Azide- and alkyne-containing fluorophore and biotin reporters are also shown (bottom).

BONCAT (bio-orthogonal noncanonical amino acid tagging),[6a,8] which uses the known methionine surrogates azidohomoalanine (AHA) and homopropargylglycine (HPG) for metabolic incorporation into newly synthesized proteins (Scheme 1, blue) and the corresponding alkyne- or azide-modified biotin reporter (Scheme 1, bottom) for subsequent proteome isolation. To monitor dynamic changes of an PTM event, we fed growing cells with an azide- or alkyne-containing sugar, fatty acid, or lipid building block (Scheme 1, orange).[6b,c] It should be noted that while our work was in progress, Hang and co-workers reported a tandem labeling and detection method to monitor the dynamic acylation of LCK (a tyrosine kinase) and its turnover.[9] Their work focused on the study of single PTM events (i.e. protein palmitoylation) of a specific protein (i.e., LCK) in a proteome. The work herein, while conceptually similar, greatly expands the scope of this double metabolic incorporation strategy by successfully demonstrating, for the first

[*] K. Liu, P.-Y. Yang, Z. Na, Prof. Dr. S. Q. Yao
Departments of Chemistry and Biological Sciences
National University of Singapore
3 Science Drive 3, Singapore 117543 (Singapore)
Fax: (+65) 6779-1691
E-mail: chmyaosq@nus.edu.sg
Homepage: http://staff.science.nus.edu.sg/~syao

[**] Technical support from Jigang Wang for LCMS experiments is acknowledged. Funding support was provided by the Agency for Science, Technology, and Research (R-143-000-391-305), Ministry of Education (R-143-000-394-112), and the National Research Foundation (Competitive Research Programme R143-000-218-281) of Singapore.

Supporting information for this article is available on the WWW under http://dx.doi.org/10.1002/anie.201102542.

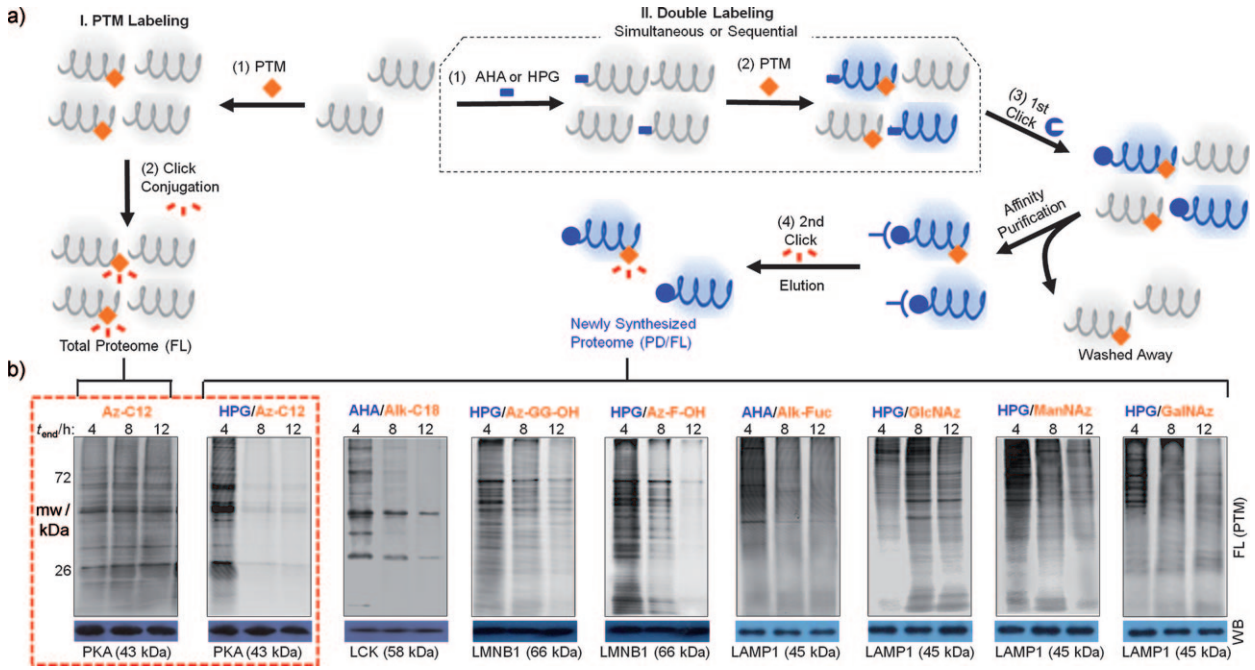

Figure 1. Double metabolic incorporation strategy for proteome-wide PTM profiling of newly synthesized proteomes. a) Overall flow of the strategy. b) Dynamic monitoring of eight PTMs on newly synthesized proteomes (AHA/HPG feeding: 1 h; PTM probe feeding: three 4 h windows (0–4, 4–8, and 8–12 h), where t_{end} represents the end time). Each experiment was conducted in duplicate to ensure reproducibility. Top: Fluorescence (FL) gels detecting PTM incorporation and profiles. Bottom: Western blotting (WB) of the same gel to ensure that newly synthesized proteins in three different lanes (t_{end} = 4, 8, 12) remained at a constant level during isolation and loading onto the gel. Each type of PTM was represented by a key protein (PKA for myristoylation, LCK for palmitoylation, LMNB1 for prenylation, LAMP1 for glycosylation). Red box: Representative examples of myristoylation showing significant differences in the PTM profiles between the total proteome and the newly synthesized proteome. PD = pull-down. See Figure S5 in the Supporting Information for full details.

time, simultaneous monitoring of PTM dynamics on multiple newly synthesized proteins (at the proteome scale) and against different types of PTMs (eight in total). As a result, unique primary PTM changes caused by external stimuli may be discovered. By further applying this improved strategy to monitor PTM changes of newly synthesized proteomes in Jurkat cells, we discovered, for the first time, that the up-regulation of myristoylated protein kinase A (PKA; a key signaling enzyme) was intimately linked to butyric acid (BA) induced apoptosis.

In our double-incorporation strategy (Figure 1), growing Jurkat cells were fed first with AHA/HPG at a predefined protein synthesis window (blue bars, step 1), then again with a desired "unnatural" PTM probe (step 2, orange diamonds in Figure 1 a) Next, a copper-catalyzed azide–alkyne [3+2] cycloaddition reaction (i.e., first click) was used to label the newly synthesized proteins with a biotin reporter. Subsequent affinity isolation separated the newly synthesized proteome using avidin agarose beads (step 3). "Old" proteins (gray in Figure 1 a), either post-translationally modified or unmodified, were removed at this stage. A subsequent on-bead (second) click reaction (step 4; with a fluorophore reporter), elution, and SDS-PAGE analysis enabled the fluorescence visualization and quantitative analysis of any PTM event that might have occurred on these newly synthesized proteins. The double incorporation of AHA/HPG and PTM probes may be carried out either simultaneously or sequentially.

To obtain optimized protocols suitable for the double incorporation strategy and subsequent proteomic studies, we first determined the optimal concentration and time needed for metabolic incorporation of AHA/HPG in Jurkat cells (Figures S1 and S2 in the Supporting Information); treatment of the cells with either 0.5 mM AHA/HPG in 10 min or 50 μM in 2 h showed that sufficient and comparable amounts of newly synthesized proteins could be obtained. Concurrent addition of cycloheximide (CHX, a protein synthesis inhibitor) during AHA/HPG feeding windows served as a convenient means to monitor and quantify newly synthesized proteomes from the resulting fluorescence gel, while the corresponding Coomassie-stained gel (which detects the complete proteome) ensured that equal total amounts of proteins were loaded and compared across different gel lanes. The AHA- or HPG-labeled, newly synthesized proteomes were shown to retain at least 80% of their total original fluorescence intensities after 48 h (Figure S3 in the Supporting Information), thus indicating that their overall recycling rate was insignificant in our assay windows. We also determined the incorporation efficiency of eight different PTM probes (structures shown in Scheme 1) covering major protein PTM events: glycosylation, acylation (palmitoylation and myristoylation), and prenylation (farnesylation and geranylation). Results showed that with 50 μM of a probe, as little as 4 h was sufficient to detect incorporation on major protein bands for most PTM events (Figure S4 in the

Supporting Information). PTM probe incorporation normally reached saturation after one day of feeding. Increasing probe dosage correspondingly shortened the time needed to achieve the same level of PTM incorporation. No apparent cytotoxicity was observed with any of the probes at our tested concentrations (Figure S10 in the Supporting Information). Large-scale pull-down and LC-MS/MS experiments were subsequently carried out to enrich these post-translationally modified proteins and unambiguously confirm their protein identities (Table S1 in the Supporting Information); upon PTM probe incorporation, proteins were labeled with the corresponding biotin probe by click chemistry, affinity-purified on avidin agarose beads, and separated by SDS-PAGE. Subsequent LC-MS/MS analysis of gel slices led to the identification of a total of 177 post-translational modifications on 112 different proteins (some proteins have more than one PTM). On average, the identification rate was about 22.1 modifications for each of the eight pull-down experiments. These proteins were then cross-checked with the literature. We confirmed a total of 71 modifications on 44 unique proteins with high confidence (that is, their PTM had previously been documented). It should be noted that our main goal was not to exhaustively identify or validate unknown PTMs. Therefore, only previously identified, high-confidence PTMs were listed (in Table S1 in the Supporting Information) and selected protein targets (i.e. LCK and PKA) were chose for more extensive investigation.

We next carried out double metabolic incorporation using all eight pairs of AHA/HPG–PTM probe combinations and studied PTM dynamics on newly synthesized proteomes (Figure 1b). The most important feature of our double incorporation strategy is the ability to artificially "fix" a protein synthesis window while "varying" the timing of PTM. In doing so, we were able to quantitatively analyze the same pool of proteins at different intervals of a PTM event during the cellular process (e.g., comparing different lanes in each fluorescence gel in Figure 1b). Thus, a potentially more accurate picture of PTM dynamics could be depicted. Briefly, protein lysates were obtained from cells treated with a one-hour feeding of AHA or HPG (0.2 mM) and each of three successive four-hour feedings with each of the eight PTM probes (0.2 mM; 0–4, 4–8, and 8–12 h, where $t = 0$ at start of AHA/HPG feeding). After sequential click chemistry, affinity purification, and gel separation, PTM profiles of these newly synthesized proteomes were rendered visible by in-gel fluorescence scanning (Figure 1b, top); each fluorescent band may be assigned to a unique protein undergoing a specific type of post-translational modification. Equal protein loading in each lane was assured by Western blotting of the same gel (Figure 1b, bottom). Striking differences were observed between PTM profiles of the total proteome and the newly synthesized proteome; representative examples of myristoylation profiles were shown in Figure 1b (red box). This example highlights the key advantage of our strategy over existing pulse-chase, isotope-based labeling methods: its ability to isolate and amplify newly synthesized proteomes and their changes, which are normally undetectable in complete proteomes.[4,5] Further quantitative fluorescence analysis of major fluorescent bands from each PTM event revealed different levels of temporal control on newly synthesized proteins (data not shown); most PTM probes, except GlcNAz, displayed the highest incorporation in the first four-hour window upon protein synthesis, then gradually stopped in the subsequent two four-hour windows, thus indicating that most PTMs occurred quite rapidly as soon as the protein synthesis was complete. The most clear-cut temporal regulation was observed with the myristoylation profile, which showed little or no detectable Az-C12 incorporation after the first four-hour window, corroborating well with the cotranslational nature of this type of PTM. Closer inspection of different bands in each gel also revealed dissimilar dynamic profiles amongst proteins undergoing the same type of PTM.

We further obtained a more detailed profile of palmitoylation dynamics by repeating the AHA/Alk-C18 double incorporation experiment with newly synthesized proteomes fed with 0.5 mM of AHA for 10 min, then with 0.5 mM of Alk-C18 for 20 min ending at nine different time points (20, 40, and 60 min and 2, 4, 8, 24, 48, and 72 h after protein synthesis). Prior to affinity purification, the complete proteome (including both "old" and newly synthesized proteins) displayed very similar palmitoylation profiles across the nine 20 min palmitoylation windows (Figure 2a, right). Upon affinity enrichment of only the newly synthesized proteome and in-gel fluorescence scanning, the resulting palmitoylation profiles revealed significant differences for different proteins across the different 20 min windows (Figure 2a, left). To further delineate the palmitoylation dynamics of each protein target, eight distinct fluorescent bands, one of which was unambiguously validated to be LCK (see WB gels in Figure S6 in the Supporting Information), were quantified and graphically plotted (Figure 2b). Even among only these proteins, highly diverse palmitoylation profiles were already evident. Rapid palmitoylation was observed for six of the eight protein bands, most of which peaked within 20 to 40 min after protein synthesis and dropped to almost undetectable levels after 2 h. In contrast, enduring palmitoylation was observed for the two remaining protein bands.

LCK is a well-known *N*-myristoylated and *S*-palmitoylated nonreceptor tyrosine kinase, whose membrane localization has profound biological implications.[9] We were interested to know whether the observed palmitoylation dynamics of newly synthesized LCK from our double incorporation strategy is related to this protein's membrane association kinetics. To determine the subcellular localization changes of newly synthesized LCK, newly synthesized proteomes were isolated from the membrane and soluble fractions of Jurkat cells, analyzed (Figure 2c), and compared with the accumulated palmitoylation counts obtained from Figure 2b. As shown in Figure 2d, within one hour after protein synthesis, the increase of the membrane-associated LCK indeed coincided quite well with palmitoylation dynamics observed. It should be highlighted that our findings herein would not have been possible if we had not isolated and analyzed only the newly synthesized proteome. We concluded that this double incorporation strategy enables proteome-wide dynamic profiling of PTMs on newly synthesized

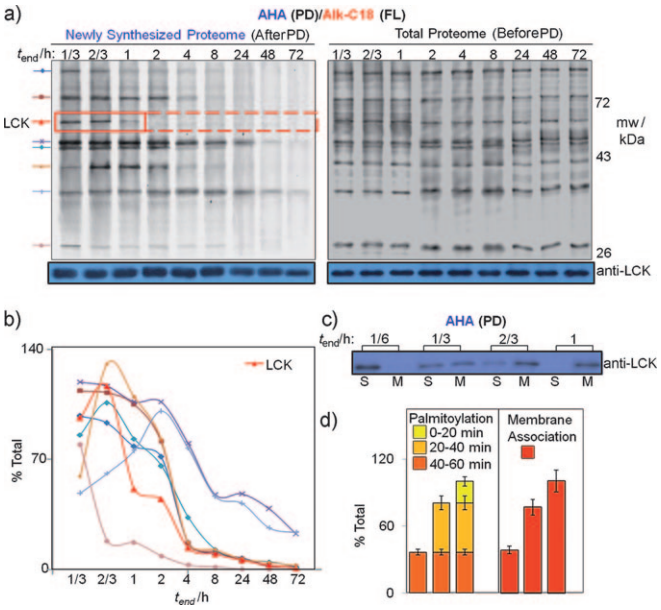

Figure 2. Monitoring the palmitoylation dynamics of newly synthesized proteomes. a) Comparison of the palmitoylation profiles (FL) generated from newly synthesized proteomes (left) and total proteomes (right), as obtained from double incorporation experiments (AHA: 10 min; Alk-C18: nine 20 min windows). The fluorescence intensity of the highlighted eight major bands is plotted in (b). The band corresponding to LCK was unambiguously validated by WB with anti-LCK antibody. Each of the other protein bands was characterized and tentatively assigned a unique protein identity from the corresponding silver-stained gel and MS/MS analysis (Figure S6 in the Supporting Information). In the newly synthesized proteome (left), bands corresponding to LCK are highlighted with a red box. WB analysis (bottom) confirmed equal amounts of LCK protein expression in each lane, despite obvious differences in fluorescence intensities, which represent different levels of LCK palmitoylation (top; red box). b) Quantitative analysis of eight different palmitoylated targets identified from the newly synthesized proteome shown in (a). The fluorescence intensity of each band from the newly synthesized proteome was quantified and divided by that from the total proteome, then plotted. This analysis produced a ratio of a newly synthesized protein's palmitoylation count to that of the all proteins over the described period after the protein was synthesized. Line graphs with error bars calculated from duplicated experiments revealing the palmitoylation change for each protein target are shown in Figure S7 in the Supporting Information. c) Membrane association dynamics of newly synthesized LCK. Lysates from cells with incorporated AHA were separated into soluble (S) and membrane (M) fractions, affinity-purified to isolate newly synthesized proteomes, and immunoblotted with anti-LCK antibody. Cells were collected at 10, 20, 40, or 60 min after addition of AHA and analyzed in lanes 1/2, 3/4, 5/6, and 7/8, respectively. d) Comparison of palmitoylation dynamics of newly synthesized LCK with its membrane association within 60 min of protein synthesis. Left: Relative percentage of cumulative palmitoylation level of LCK as obtained from (b). Right: Relative percentage of membrane-associated LCK as obtained from (c). Each experiment was conducted in duplicate to ensure reproducibility. Error bars were generated from duplicated experiments. See the Supporting Information for details.

proteomes. By adjusting metabolic feeding windows, the strategy is applicable to both rapid and enduring PTM events.

Lastly, we explored the feasibility of this approach to discover novel PTM regulations on newly synthesized proteomes. It is known that butyric acid (BA) induced protein synthesis in Jurkat cells is critical for apoptosis to occur, but to date the molecular basis of this process is not well understood.[10] We were interested to know whether the dynamic PTM regulation of any of the newly synthesized proteins might play a role in the early stage of apoptotic induction. By applying the double incorporation strategy (HPG/Az-C12) to BA-treated cells in the 0–5 h window with subsequent sequential click chemistry (HPG labeled with Az-Biotin, Az-C12 labeled with Alk-Alx), enrichment of newly synthesized proteomes, and in-gel fluorescence scanning, we obtained the corresponding myristoylation profiles (with and without myristoylation inhibitor HMA; lanes 5 and 6, respectively, in the center gel in Figure 3a) as well as those of the corresponding total proteomes (i.e., before avidin pull-down; left gel). A close examination of the newly synthesized proteomes revealed a significant fluorescence increase in a 43 kDa band (labeled with an asterisk in Figure 3a) only in the BA-treated proteome. This 43 kDa protein was subsequently identified to be myristoylated PKA catalytic subunit alpha (PRKACA) by immunoprecipitation (IP) and immune-depletion (ID) experiments (right gel in Figure 3a). Further quantitative analysis was carried out on this fluorescent band (indicating PKA myrisoylation counts) and its Western-blotted counterpart (indicating PKA expression counts) for both the complete proteomes and the newly synthesized proteomes (Figure 3b); up-regulation of both the myristoylated PKA and overall PKA expression was clearly evident in the newly synthesized proteomes (right) but not in the total proteomes (left). Under our assay conditions, the newly synthesized proteome made up only a small fraction of the total proteome. This situation might have obscured the detection of PKA up-regulation in the total proteome of BA-induced apoptotic cells. Protein myristoylation is normally a cotranslational event, and PKA myristoylation has been postulated to be involved in modulation of its translocation and membrane association.[11] As a key signaling enzyme involved in energy metabolism, PKA might play a vital role in controlling BA-induced apoptosis of Jurkat cells by up-regulation of its expression level, which leads to myristoylation and subsequent modulation of its enzymatic activity.[12] To confirm this hypothesis, we determined the effect of H89 (a PKA inhibitor), HMA (a myristoylation inhibitor), and siRNA of PKA in blocking BA-induced apoptosis (Figure 3d,e). DNA fragmentation assay revealed that only a combined H89 + HMA treatment, or siRNA knockdown of PKA, was able to sufficiently block BA-induced apoptosis, but not H89 or HMA alone or scrambled siRNA (Figure 3d). A time-dependent assay lends further support to our observations (Figure 3e), thus unequivocally demonstrating that up-regulation of myristoylated PKA is needed for the occurrence of BA-induced apoptosis in Jurkat cells.

In summary, our double metabolic incorporation approach was capable of proteome-wide monitoring of PTM dynamics on newly synthesized proteins. The novelty of this approach is the ability to enrich newly synthesized proteins from a predefined time window, then progressively monitor their post-translational modifications over time by

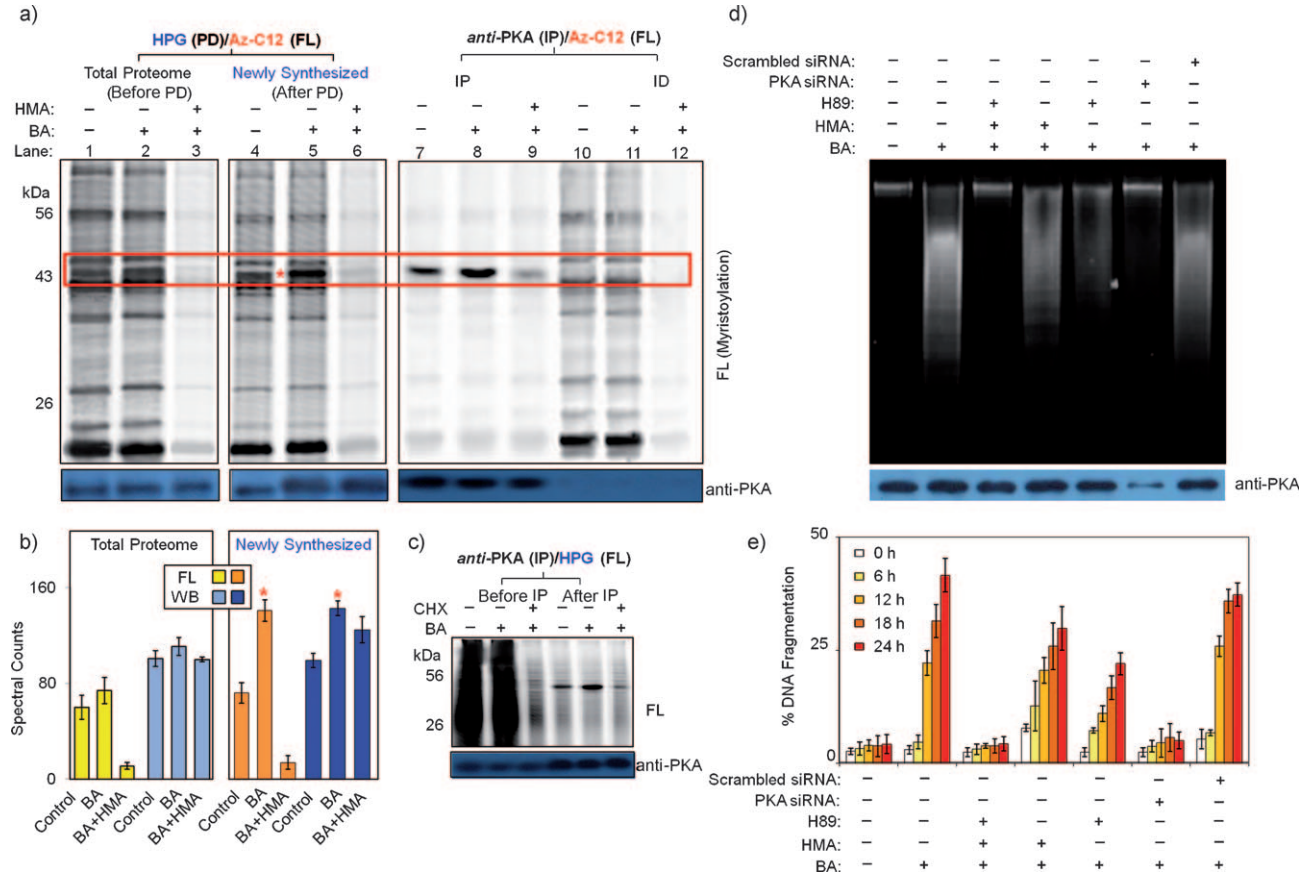

Figure 3. Identification of up-regulated myristoylated PKA at the early stage (0–5 h after addition of BA) of BA-induced apoptosis. a) Comparing myristoylation profiles of the total proteome (left) and newly synthesized proteome (middle). In each gel, control lanes were obtained from cells treated with or without different BA/HMA combinations (HMA is a myristoylation inhibitor). BA (5 mM) was added to growing Jurkat cells. Double incorporation was carried out by simultaneously feeding the cells with HPG (50 μM) and Az-C12 (0.2 mM) during 0–5 h. Newly synthesized proteomes were separated from total proteomes by click labeling and affinity pull-down (PD). Myristoylation profiles of the proteomes were visualized by fluorescence tagging. Right: Validation of the 43 kDa band as myristoylated PKA catalytic subunit alpha by immunoprecipitation (IP) and immune-depletion (ID) with anti-PKA. To aid the view, the 43 kDa band corresponding to PKA in all three gels is highlighted in a red box. Western blotting results with anti-PKA are shown below each gel. b) Quantitative analysis of the 43 kDa PKA bands from the left and center gels in (a). Both the myristoylation counts (FL) and PKA expression count (WB) between the total proteome (left) and the newly synthesized proteome (right) were plotted. *: up-regulation of myristoylated PKA only became evident in the BA-treated, newly synthesized proteome. Means ± standard errors were obtained from duplicates. c) Validation of PKA's up-regulation in newly synthesized proteomes. BA-treated cells were fed with HPG and fluorescently labeled. After immunoprecipitation (IP) with anti-PKA (lanes 4–6), noticeable up-regulation of newly synthesized PKA in lane 5 was evident (compared to lane 4). d) DNA fragmentation assay showing effects of H89 + HMA combination and siRNA knockdown of PKA in blocking BA-induced apoptosis. Western blotting analysis of the corresponding protein samples with anti-PKA reveals the knock-down of PKA expression by PKA siRNA but not by scrambled siRNA. e) Time-dependent BA-induced apoptosis and its inhibition by H89 + HMA combination or by siRNA knockdown of PKA. Each experiment was conducted in duplicate to ensure reproducibility. Means ± standard errors were obtained from duplicates. See the Supporting Information, Figure S9, for further control experiments.

quantitative in-gel fluorescence scanning. This approach is different from the work by Hang and co-workers, where newly synthesized proteomes were not isolated and only a limited number of PTMs (i.e., myristoylation and palmitoylation) was demonstrated. With our strategy, we identified for the first time that up-regulation of myristoylated PKA catalytic subunit alpha is necessary for the occurrence of butyric acid induced apoptosis in Jurkat cells. Work is underway to identify downstream targets of PKA and to further expand the utility of this new chemical proteomic tool with other powerful mass spectrometric techniques such as ICAT (isotope coded affinity tagging) and SILAC (stable isotope labeling by amino acids in cell culture).[13]

Received: April 12, 2011
Published online: June 15, 2011

Keywords: apoptosis · click chemistry · metabolic incorporation · post-translational modification · proteins

[1] C. T. Walsh, S. Garneau-Tsodikova, G. J. Gatto, Jr., *Angew. Chem.* **2005**, *117*, 7508–7539; *Angew. Chem. Int. Ed.* **2005**, *44*, 7342–7372.
[2] M. Mann, O. N. Jensen, *Nat. Biotechnol.* **2003**, *21*, 255–261.
[3] a) W. P. Heal, E. W. Tate, *Org. Biomol. Chem.* **2010**, *8*, 731–738, and references therein; b) H. C. Hang, C. Yu, D. L. Kato, C. R. Bertozzi, *Proc. Natl. Acad. Sci. USA* **2003**, *100*, 14846–14851;

c) T. L. Hsu, S. R. Hanson, K. Kishikawa, S. K. Wang, M. Sawa, C. H. Wong, *Proc. Natl. Acad. Sci. USA* **2007**, *104*, 2614 – 2619; d) H. C. Hang, E. J. Geutjes, G. Grotenbreg, A. M. Pollington, M. J. Bijlmakers, H. L. Ploegh, *J. Am. Chem. Soc.* **2007**, *129*, 2744 – 2745; e) B. R. Martin, B. F. Cravatt, *Nat. Methods* **2009**, *6*, 135 – 138; f) M. A. Kostiuk, M. M. Corvi, B. O. Keller, G. Plummer, J. A. Prescher, M. J. Hangauer, C. R. Bertozzi, G. Rajaiah, J. R. Falck, L. G. Berthiaume, *FASEB J.* **2008**, *22*, 721 – 732; g) B. S. Davies, S. H. Yang, E. Farber, R. Lee, S. B. Buck, D. A. Andres, H. P. Spielman, B. J. Agnew, F. Tamanoi, L. G. Fong, S. G. Young, *J. Lipid Res.* **2008**, *50*, 126 – 134.

[4] a) I. Kratchmarova, B. Blagoev, M. Haack-Sorensen, M. Kassem, M. Mann, *Science* **2005**, *308*, 1472 – 1477; b) S. Matsuoka, B. A. Ballif, A. Smogorzewska, E. R. McDonald III, K. E. Hurov, J. Luo, C. E. Bakalarski, Z. Zhao, N. Solimini, Y. Lerenthal, Y. Shiloh, S. P. Gygi, S. J. Elledge, *Science* **2007**, *316*, 1160 – 1166; c) H. Daub, J. V. Olsen, M. Bairlein, F. Gnad, F. S. Oppermann, R. Korner, Z. Greff, G. Keri, O. Stemmann, M. Mann, *Mol. Cell* **2008**, *31*, 438 – 448.

[5] S. Pedersen, P. L. Bloch, S. Reeh, F. C. Neidhardt, *Cell* **1978**, *14*, 179 – 190.

[6] a) J. A. Johnson, Y. Y. Lu, J. A. Van Deventer, D. A. Tirrell, *Curr. Opin. Chem. Biol.* **2010**, *14*, 774 – 780; b) N. J. Agard, C. R. Bertozzi, *Acc. Chem. Res.* **2009**, *42*, 788 – 797; c) R. N. Hannoush, J. L. Sun, *Nat. Chem. Biol.* **2010**, *6*, 498 – 506.

[7] E. M. Sletten, C. R. Bertozzi, *Angew. Chem.* **2009**, *121*, 7108 – 7133; *Angew. Chem. Int. Ed.* **2009**, *48*, 6974 – 6998.

[8] a) D. C. Dieterich, A. J. Link, J. Graumann, D. A. Tirrell, E. M. Schuman, *Proc. Natl. Acad. Sci. USA* **2006**, *103*, 9482 – 9487; b) K. E. Beatty, J. C. Liu, F. Xie, D. C. Dieterich, E. M. Schuman, Q. Wang, D. A. Tirrell, *Angew. Chem.* **2006**, *118*, 7524 – 7527; *Angew. Chem. Int. Ed.* **2006**, *45*, 7364 – 7367; c) G. Kramer, R. R. Sprenger, J. Back, *Mol. Cell. Proteomics* **2009**, *8*, 1599 – 1611; d) D. C. Dieterich, J. L. Hodas, G. Gouzer, *Nat. Neurosci.* **2010**, *13*, 897 – 905; e) R. B. Deal, J. G. Henikoff, S. Henikoff, *Science* **2010**, *328*, 1161 – 1164.

[9] M. M. Zhang, L. K. Tsou, G. Charron, A. S. Raghavan, H. C. Hang, *Proc. Natl. Acad. Sci. USA* **2010**, *107*, 8627 – 8632.

[10] V. Medina, B. Edmonds, G. P. Young, R. James, S. Appleton, P. D. Zalewski, *Cancer Res.* **1997**, *57*, 3697 – 3707.

[11] C. Breitenlechner, R. A. Engh, R. Huber, V. Kinzel, D. Bossemeyer, M. Gassel, *Biochemistry* **2004**, *43*, 7743 – 7749.

[12] a) M. J. Bijlmakers, M. Marsh, *Trends Cell Biol.* **2003**, *13*, 32 – 42; b) R. Franklin, J. McCubrey, *Leukemia* **2000**, *14*, 2019 – 2034.

[13] a) S. P. Gygi, B. Rist, S. A. Gerber, F. Turecek, M. H. Gelb, R. Aebersold, *Nat. Biotechnol.* **1999**, *17*, 994 – 999; b) S. E. Ong, I. Kratchmarova, M. Mann, *J. Proteome Res.* **2003**, *2*, 173 – 181.

